Formation, stability, and mobility of self-trapped excitations in NaI and $NaI_{1-x}Tl_x$ from first principles

M. P. Prange,[1] R. M. Van Ginhoven,[2] N. Govind,[3] and F. Gao[1]

[1]*Fundamental and Computational Sciences Directorate, Pacific Northwest National Laboratory, Richland, Washington 99352, USA*

[2]*Energy and Environment Directorate, Pacific Northwest National Laboratory, Richland, Washington 99352, USA*

[3]*William R. Wiley Environmental Molecular Sciences Laboratory, Pacific Northwest National Laboratory, Richland, Washington 99352, USA*

(Received 9 August 2012; revised manuscript received 4 February 2013; published 4 March 2013)

We study the formation, mobility, and stability of self-trapped excitons (STE) and self-trapped holes and electrons in NaI and NaI(Tl) using embedded cluster hybrid density functional theory calculations. This method employs an array of classical charges to provide an environment simulating the interior of an ionic solid in which the electronic structure of a modestly sized quantum-mechanical cluster is computed including nonlocal exchange effects which are necessary to describe localized excitations in NaI. In contrast with previous models, we find that both carriers in pure NaI have similar mobilities, with an activation energy of $\sim$0.2 eV. We propose an alternate interpretation including a new migration mechanism for the STE. In Tl-doped material excitons preferentially trap at dopants, inducing off-center distortions that have a structure unlike an STE and provide a mechanism for light emission at multiple wavelengths.

DOI: 10.1103/PhysRevB.87.115101 PACS number(s): 71.35.Cc, 71.35.Aa, 72.20.Ee, 72.20.Jv

I. INTRODUCTION

Recent progress in multiscale modeling of scintillating radiation detectors shows great promise.[1] Such efforts, however, require a *quantitative* understanding of all relevant microscopic processes which can then be correctly parametrized in meso- or macroscale models. While some quantities are accessible by measurement, the picture is often incomplete and sometimes qualitatively incorrect. This paper presents results using first-principles calculations that capture important details of the microscopic physics of NaI that are crucial to understanding and modeling of detector performance.

Thallium-doped NaI is of particular interest because it is widely used and the standard material against which new scintillators are compared.[2] In scintillation radiation detection, highly energetic radiation causes a cascade of secondary excitations in the crystal. Some of these excitations ultimately relax by the emission of visible light which is measured as a proxy for the energy of the incident radiation. The energy resolution of scintillators is limited by the nonproportionality of light yield to incident energy.[3]

Despite decades of experimental[4–8] and theoretical[5,9–12] study, microscopic understanding of the competing modes of energy transport and conversion in alkali halides is incomplete, and the interaction of energy carriers with dopants is only partially understood. Experimental and theoretical studies show that the luminescence efficiency depends on the spatial distribution of the secondary excitations, with higher densities of excitations producing fewer luminescence photons per unit deposited energy for low excitation energies.[3,13–15] This falloff of luminescence efficiency at low energies and high excitation densities is common in scintillators but especially pronounced in NaI(Tl). It is attributed to quenching of the secondary excitations by nonradiative processes that leave the energy carried by a pair (or more, for higher order processes) of secondary excitations in the vibrational modes of the scintillator and hence unavailable for luminescence.

We address the formation and diffusion of holes and excitons in pure and Tl-doped NaI, which are the important secondary excitations for luminescence. Self-trapped holes (STHs) (V_k centers) consist of a missing electron in a valence band and an accompanying strong lattice distortion, and a self-trapped exciton (STE) can be thought of as an STH surrounded by a bound electron. In both cases the lattice relaxation in the pure material resembles the formation of an I_2^- ion within the bulk crystal[16] with two I atoms moving markedly together. Such self-trapped excitations were qualitatively explained theoretically by the 1970s,[17,18] but improvement of theoretical understanding is ongoing, and a fully detailed description has not yet been achieved.[19,20]

During a scintillation event in NaI or NaI(Tl), these self-trapped excitations are initially created in a track, the structure of which depends on the particular exciting radiation. After creation, the self-trapped excitations execute diffusive motion until their decay. In the Tl-doped material, the dominant mechanism for light emission is STE capture by a Tl dopant (activator) followed by photon emission by the Tl. In the absence of such activator sites, the dominant process for light emission is direct radiative decay of STEs. The dominant quenching mechanism is STE-STE annihilation, in which two excitons collide and are destroyed. In both cases, light emission involves a single STE and hence depends linearly on the STE density while the quenching mechanism, which requires (at least) a binary collision, depends on higher powers of the excitation density leading to decreased luminescence efficiency at high excitation densities. Meanwhile, STHs and free carriers are also produced in the track. They can combine to form excitons (including STEs) or luminescence photons. Thus, a detailed understanding of scintillator performance in these systems requires understanding of the motion of STEs, free electrons, and STHs in order to predict the time evolution of the populations of each type of excitation and their ultimate fates. Various attempts have been made to describe scintillation efficiency by modeling the time and spatial dependence of secondary excitations using Monte-Carlo approaches, models based on rate equations, or ones based on diffusion equations. These are reviewed in Ref. 13. All these approaches are

limited by the paucity of knowledge regarding the microscopic dynamics of low-energy excitations.

Previously proposed models,[15,21] based on optical experiments,[22,23] assumed a highly mobile STE and a slower STH, while we find that in pure NaI both carriers have similar mobilities, with an activation energy of $\sim$0.2 eV. We propose an alternate interpretation, in which an electron hops from an STE to an STH at a different site, effectively exchanging the STE and STH. Our calculations suggest this migration mechanism should have a much lower barrier, consistent with measurements. Excitons migrating via this mechanism are likely to exhibit dynamics with different dependencies on temperature and local excitation density than excitons migrating by the conventional hopping mechanism. Importantly for theories of scintillation efficiency, STEs hopping by this mechanism can-not participate directly in STE-STE annihilation, since the destination site for this mechanism must contain an STH. Hence the existence of two different hopping barriers has implications for detector nonproportionality.

As is well known, accurate calculations of localized states in alkali halides are challenging because density functional theory (DFT) using semilocal exchange-correlation potentials often provides a qualitatively incorrect picture [e.g., neither STEs nor STHs are stable compared to undistorted structures in NaI (Ref. 24)]. To circumvent this problem we employ hybrid DFT with nonlocal exchange.

Most previously reported calculations on alkali halide systems (e.g., Refs. 25, 10, and 11) have been performed using some form of pure Hartree Fock (HF) theory. Notable exceptions are Derenzo and Weber[26] and Rivas-Silva *et al.*[27] who used MP2 and QCISD levels of theory, respectively, to calculate emission energies. These previous works relied on small or symmetry constrained models to improve calculation tractability or to explore a specific proposed geometry. Since confinement effects limit the deformations available, small clusters discourage localized states which involve such distortion or lattice polarization. On the other hand, the use of pure HF, which completely neglects the correlation energy, favors localized states. Hence there is the possibility that these two errors partially cancel leading to qualitatively correct results. This work (with as many as 136 *ab initio* atoms and no constraints on the symmetry of the deformation) is a substantial improvement over previous efforts in this area.[10,11,25–27]

II. COMPUTATIONAL METHODS

As in past work,[11,17,18,28,29] we use an embedded cluster method to facilitate tractable calculations. Our calculations include a large ($\sim$10 000) array of fixed point charges, located at lattice positions of the undistorted crystal. This array provides an electrostatic potential which closely reproduces the classical Ewald potential of the perfect crystal throughout a central region in the interior of the array. The atoms on surface of the cluster are fixed throughout the calculation, and the interior atoms are allowed to relax. A schematic diagram of a cluster model is shown in Fig. 1.

Within the quantum-mechanical region, the electronic structure was computed by means of hybrid DFT using CRENBL ECP (Ref. 31) basis sets for Na and I and Stuttgart RLC basis sets[32] for Tl. Unless otherwise stated,

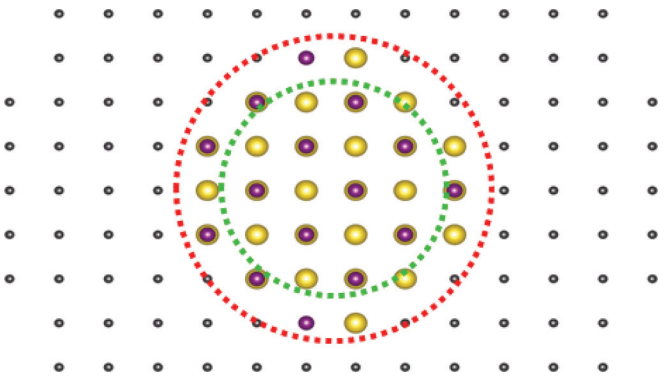

FIG. 1. (Color online) Cutaway view of embedded cluster model of NaI. Classical charges are shown in gray, Na atoms in gold, and I atoms in purple. In this model there are 16 248 charges and 136 atoms. Atoms within the inner circle are allowed to relax during geometry optimization, while those atoms between the circles are held fixed. This image and all images in this paper depicting structures were created using VESTA (Ref. 30).

the cluster models contained 136 quantum-mechanical atoms. The positions of 51 of these were varied in the optimizations. For each Na atom in the cluster two electrons were treated by means of an effective core potential. For each I, 46 electrons were so treated. The calculations presented here are scalar ones that do not include the spin-orbit interaction. The Becke half-and-half[33] (BHH) exchange-correlation potential was used. Unless otherwise stated, calculations were carried out using the NWCHEM code.[34]

III. RESULTS

A. Pure NaI

To characterize localized excitations we constrained the number of spin-up and spin-down electrons and searched for the nuclear coordinates that minimized the total energy of the cluster model subject to these constraints. The results of such a procedure are the geometry and energy of the lowest energy state of each type: a doublet of charge +1 in the case of the STH and a neutral triplet in the STE case. We find that on-center self-trapped holes and excitons are stable in NaI compared to delocalized states, but electrons do not self-trap in pure NaI clusters in our calculations even for pure HF which is known to favor self-trapped states.[20]

In our models, the two I atoms participating in the STE are separated by 3.36 Å, close to the measured (3.23 Å)[35] and theoretical (3.31 Å) isolated I_2^- bond length and far from the I-I separation in the undistorted NaI crystal (4.58 Å). Our isolated I_2^- bond length is in good agreement with other calculations,[36] and the actual STE I-I separation is also in agreement with other theoretical results.[37] The energy of the STE is calculated to be 5.68 eV above the (singlet) ground state of the undistorted crystal and 0.7 eV below the lowest energy triplet state of the undistorted crystal. The measured excitation energy is 5.61 eV.[38] In addition, we calculated an emission energy of 4.27 eV for the STE, in good agreement with the experimentally measured value of 4.207 eV.[39] We also find an on-center STH which resembles the STE (3.38 Å I-I separation) with the electron removed.

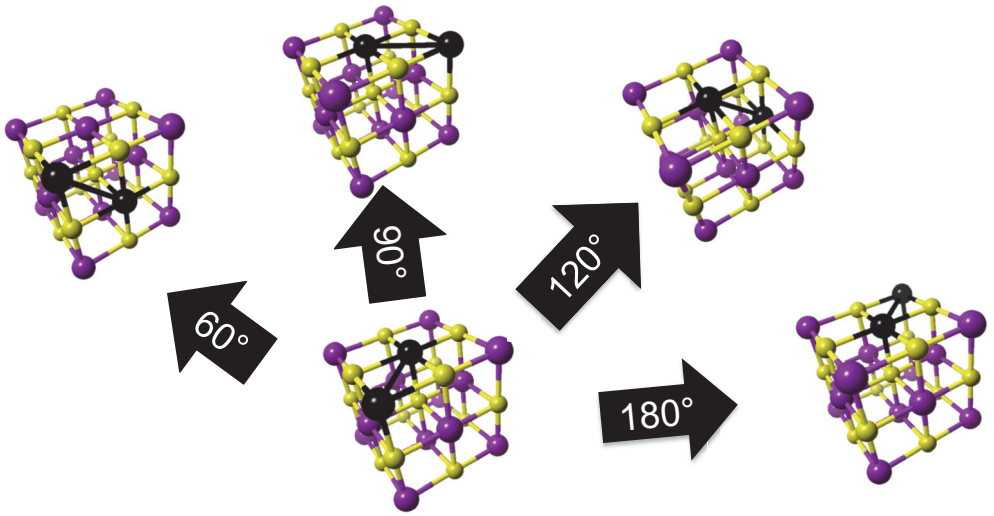

FIG. 2. (Color online) The four near-neighbor hops available to the STE or STH in NaI.

Our calculations estimate the energy of this STH to be 0.50 eV lower than a delocalized hole in the undistorted crystal.

Assuming the conventional picture in which self-trapped excitations migrate via the transfer of lattice distortion and spin density between adjacent lattice sites, we calculated the energy barrier for hopping of the STE and STH in NaI for each of the four possible hop angles between iodine neighbor pairs in the rocksalt structure which are depicted in Fig. 2.

For each hop and type of self-trapped excitation, cluster models were relaxed with the excitation positioned at either end of the jump. The transition state was estimated by relaxing the interior atoms of the cluster except the two I atoms directly participating in the self-trapped excitation (the active halogens) from a starting geometry calculated as the average of the geometries before and after the jump. We have reported this energy difference as the migration barrier in Table I. For all STH jumps, the hole orbital at the transition state is shared among the three halogens involved in the jump. Most of the orbital resides on the central I that participates in the STH before and after the jump, with smaller but significant contributions from the other two iodines involved. Previous work in other alkali halide systems has found similar transition states.[40] Shluger and co-workers[40] postulated the existence of a "one-center" self-trapped hole state near the transition state for the 60° STH jump. They found this state to be unstable; we find the same conclusion for our system in the present work. The energy difference between a one-center trapped hole and the STH provides an upper bound for the transition barrier and provides an explanation for the nearly identical barriers since any of the hops could be accomplished by first transitioning to the one-center state which appears to be adiabatically connected to all the STH states in which the single center participates.

TABLE I. Calculated migration barriers for STH and STE in pure NaI.

Hop angle (deg)	STH barrier (eV)	STE barrier (eV)
60	0.225	0.199
90	0.285	0.267
120	0.241	0.274
180	0.223	0.258

We show the spin density for the relaxed STH and for the transition state of the 120° hop in Fig. 3. In our simulations, the behavior of the hole in the STE hops is very similar to that of the hole in the corresponding STH hops. The STE electron becomes delocalized in the transition state for all hop angles in our clusters.

Popp and Murray[8] estimated a barrier of 0.18 eV for the 60° STH jump, in reasonable agreement with our value of 0.225 eV. On the other hand, experimental estimates of the STE hopping barrier are much lower. For example, Nagata and co-workers[22,23] reported 0.07 eV for Tl-doped NaI. The magnitude of this barrier is directly related to the thermally activated mobility of the STE, and our results suggest that the conventional picture of the low-energy kinetics of STEs should be reexamined. In particular, we expect, based on our calculations, the STE and STH to have nearly identical mobilities. The lower barrier ascribed to the STE can be attributed to the migration of electrons hopping from an STE to a nearby STH. Since the geometries of the STH and STE are similar, we expect the barrier for such a hop to be low. In fact the energy gained by relaxing the neutral triplet state starting in the STH geometry (so that the final configuration is an STE) is 0.02 eV. The hopping barrier can be expected to be of the same order of magnitude.

B. Tl impurities

NaI is commonly doped with Tl, which substitutes for Na at a lattice site to create a light-emitting center. The transfer of energy from diffusing self-trapped excitations to these luminescence centers, while believed to play a significant role in scintillator performance, is not well understood. To investigate this process, we simulated Tl impurities in our models. The lowest energy singlet state for our clusters involves only modest displacements around the Tl to accommodate the larger size of the dopant compared to the Na atom it replaces.

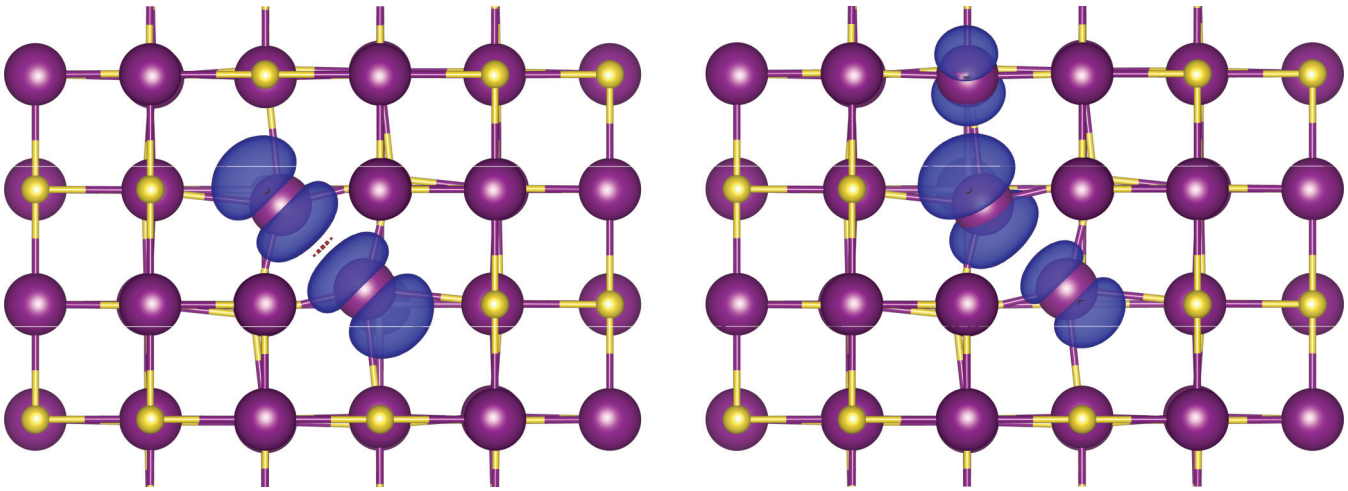

FIG. 3. (Color online) Spin density isosurfaces drawn at 0.001 electrons/bohr^3 around an STH (left panel) and the transition state for a 120° STH jump (right panel).

By optimizing the geometry from various starting points and spin populations, we find a rich collection of stable trapped excitations from this state including two distinct neutral triplet excitons as well as a single trapped hole and a trapped electron.

The two nearly degenerate (the energy of the edge configuration is higher by 0.04 eV in our model) triplet excitations are depicted in Fig. 4. We note that, unlike the bulk self-trapped excitations, the Tl-trapped excitons are stable in LDA and

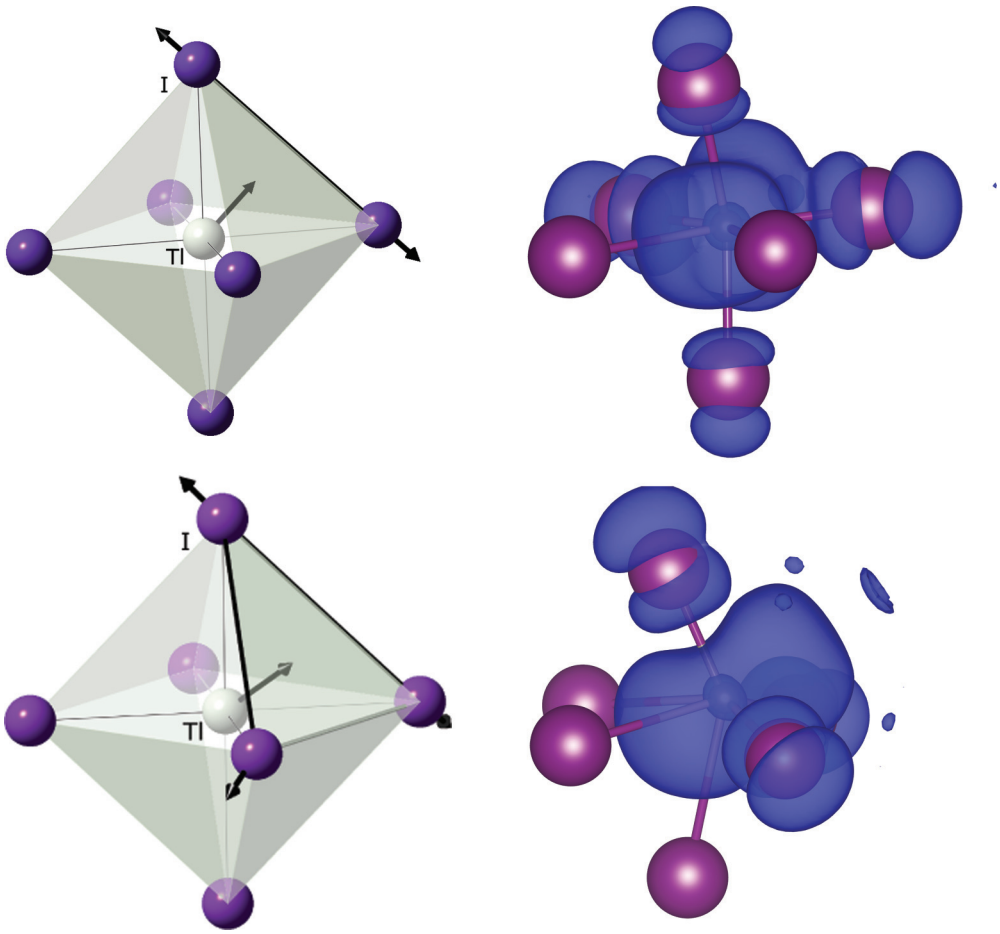

FIG. 4. (Color online) The left column shows schematic diagrams of the displacements relative to a perfect NaI crystal lattice of a Tl impurity participating in two different exciton states. The right column shows the optimized coordinates of the coordinating octahedron that holds the Tl impurity along with a spin density isosurface drawn at 0.001 electrons/bohr^3.

PBE theories, although PBE reverses the relative energies of the two excitons. In bulk NaI, each Na cation is octahedrally coordinated by I anions. The Tl in the singlet ground state sits similarly in the center of a nearly regular octahedron with I at each vertex. The relaxations accompanying the trapping of the triplet states involve the movement of the Tl towards either an edge or face of the octahedron which expands to accommodate the Tl. In both cases the spin density associated with the triplet exciton is localized on the Tl and the accommodating I atoms (cf. Fig. 4). The orbitals involved in the excitons have *s* character around the Tl and *p* character around the I atoms. Calculations of the barrier between the two Tl-trapped excitons were done using cluster models. Additionally, we used the nudged elastic band method as implemented in the SEQQUEST code[41,42] to estimate the barrier. Both LDA[43] and PBE[44] functionals were used. These calculations all indicate that the barrier is very low and that the Tl can rattle around nearly freely in the octahedron formed by the nearest iodines.

We found these Tl-trapped triplet states to be stable compared to a (bulk) STE near a singlet Tl by $\sim$0.25 eV and hence expect diffusing STEs to be trapped when they encounter Tl impurities. Even though the excited states are essentially degenerate, the excitation depicted in Fig. 4(a) has a luminescence energy of 3.46 eV, while the excitation depicted in (b) has a luminescence energy of 2.85 eV due to the slope of the ground-state potential energy surface between the excited state geometries. These calculated transition energies compare well with low-temperature experiments on NaI(Tl)[39] finding bands centered at at 3.76 and 2.95 eV. In other doped alkali halide systems these A_T and A_X emissions have similar structure.[45,46]

The off-site displacement of the Tl center is due to broken symmetry on the excited state potential energy surface induced by the presence of an electron with *p* orbital character. We expect the same type of distortion to occur for the triplet exciton, the trapped electron (Tl^0), and the singlet excited state (Tl*).

We propose that the localized triplet states depicted in Fig. 4 play a role in the transfer of energy from free, diffusing STEs to fixed luminescence centers by capturing the spin density associated with the STE and thereby destroying the STE. The distortion around the Tl, which cannot migrate, replaces the STE. We have succeeded in relaxing a lattice STE in a layer adjacent to a Tl impurity's surrounding octahedron, hence we estimate the radius for capture of a diffusing STE by a Tl impurity to be of the order of the lattice constant.

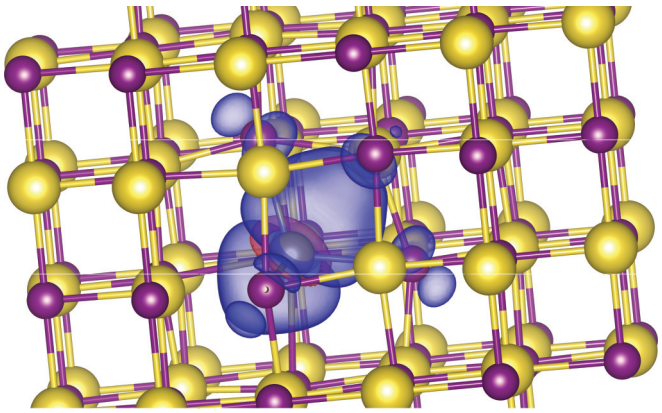

FIG. 5. (Color online) Spin density isosurface drawn at 0.0005 electrons/bohr^3 in a 136-atom cluster containing a Tl^0.

TABLE II. Bond lengths and relaxation energies (energy difference between positively charged clusters in undistorted and fully relaxed geometries) for the STH in pure NaI for several cluster models of different sizes. BHH xc was used for these calculations, so the first line of this table and Table IV are identical. The bond lengths are in Å and the energies in eV.

Cluster size	Bond length	Relaxation energy
48	3.383	0.50
80	3.371	0.69
136	3.357	0.72

Finally, we have found a shallow but stable minimum in which an electron is localized on a Tl impurity (i.e., a Tl^0). The relaxation around this state resembles the exciton in which the octahedron edge lengthens to accommodate the displacement of the Tl (the top row of Fig. 4). This Tl^0 state is only 0.1 eV lower in energy than a delocalized electron in the relaxed singlet (Tl^+) geometry. The spin density of the Tl^0 state is depicted in Fig. 5.

IV. DISCUSSION

To explore the dependence of the physics of self-trapped excitations on cluster size and exchange-correlation treatment, we varied each approximation in baseline calculations of the STH. Table II shows the bond length of the I_2^- in the STH and the relaxation energy (energy gained by allowing the I_2^- to form in a positively charged cluster) for three cluster sizes. In Table III we show various energy differences in neutral cluster models of the same size as those used in Table II. We list the energy difference between the lowest unoccupied orbital (LUMO) and the highest occupied orbital (HOMO) of the singlet configuration at the relaxed singlet (i.e., bulklike ground state) geometry. We also list the excitation energy which is computed as the difference between the total energy of the relaxed triplet (i.e., STE) geometry and the total energy of the relaxed singlet (ground state). Finally we list luminescence energies which were calculated as the difference between the triplet and singlet potential energy surfaces at the relaxed triplet (STE) geometry. From these convergence studies, we estimate the errors due to finite cluster size in energies are $\sim$0.1 eV and in bond lengths are $\sim$0.05 Å.

TABLE III. Calculated energy differences (in eV) for neutral cluster models of different sizes. We show singlet HOMO-LUMO gaps and excitation and luminescence energies for the STE.

Cluster size	HOMO-LUMO	Excitation	Luminescence
48	7.39	5.74	4.49
80	7.23	5.57	4.17
136	7.16	5.68	4.27
Experiment		5.61 (Ref. 38)	4.207 (Ref. 39)

TABLE IV. Bond length, 60° migration barriers, and relaxation energies (energy difference between positively charged clusters in undistorted and fully relaxed geometries) for the STH in pure NaI for several xc functionals which are described further in the text. All calculations in this table used identical 48-atom models. The bond lengths are in Å and the energies in eV.

Functional	60° barrier	Bond length	Relaxation energy
BHH	0.225	3.383	0.50
HF	0.193	3.370	1.55
B3LYP	0.150	3.383	−0.04
Becke 0.325 and 0.625	0.140	3.423	0.18

In Table IV we present the 60° migration barrier, bond length, and relaxation energy for the STH computed with several exchange-correlation (xc) functionals but otherwise identical cluster models. In addition to BHH (Ref. 33) (used for all other results in this paper), results obtained using B3LYP,[47] HF, and a modified BHH in which the fraction of of HF exchange is reduced from 1/2 to 0.325 are tabulated. The bond length is rather insensitive to xc treatment, but, surprisingly, the migration barrier is smaller in the HF theory than in the BHH one. The relaxation energy, however, is monotonic in the fraction of HF exchange included in the otherwise semilocal functional. In fact, the STH, while locally stable, is higher in energy than the undistorted structure in the B3LYP theory. Based on these calculations it is our opinion that in the case of ionic solids such as the alkali halides, the uncertainty in the calculated energies due to the exchange-correlation treatment is larger than that due to finite cluster size effects.

V. CONCLUSION

We have studied trapped excitations in NaI with *ab initio* hybrid DFT using large systems. We find an on-center STE and STH in the pure material and excitons trapped on Tl impurities in NaI(Tl). Our calculations are in very good agreement with available experimental data and largely consistent with the conventional picture of scintillation in NaI except for the STE hopping mobility, for which we find a much higher barrier (close to that for the STH) in our calculations. We suggest further work to validate the barriers and energy levels published here as well as a theoretical description of other microscopic properties outside the scope of this paper, such as STE-STE annihilation, and STE radiative and nonradiative decay lifetimes. It is also our hope that models of scintillation efficiency, parametrized with *ab initio* results such as the ones presented here and including both STE migration mechanisms be constructed and tested.

ACKNOWLEDGMENTS

This research was supported by the National Nuclear Security Administration, Office of Nuclear Nonproliferation Research and Engineering (NA-22), of the U.S. Department of Energy (DOE). A portion of this research was performed using EMSL, a national scientific user facility sponsored by the Department of Energy's Office of Biological and Environmental Research and located at Pacific Northwest National Laboratory. Additionally, a portion of the research was performed using PNNL Institutional Computing at Pacific Northwest National Laboratory.

[1] Z. Wang, Y. Xie, B. D. Cannon, L. W. Campbell, F. Gao, and S. Kerisit, J. Appl. Phys. **110**, 064903 (2011).
[2] G. F. Knoll, *Radiation Detection and Measurement*, 3rd ed. (Wiley, New York, 2000).
[3] R. Devanathan, L. R. Corrales, F. Gao, and W. Weber, Nucl. Instrum. Methods Phys. Res. A **565**, 637 (2006).
[4] J. C. Phillips, Phys. Rev. **136**, A1705 (1964).
[5] R. T. Williams, K. S. Song, W. L. Faust, and C. H. Leung, Phys. Rev. B **33**, 7232 (1986).
[6] K. Teegarden and G. Baldini, Phys. Rev. **155**, 896 (1967).
[7] J. E. Eby, K. J. Teegarden, and D. B. Dutton, Phys. Rev. **116**, 1099 (1959).
[8] R. Popp and R. Murray, J. Phys. Chem. Solids **33**, 601 (1972).
[9] C. H. Leung and K. S. Song, J. Phys. C **12**, 3921 (1979).
[10] A. L. Shluger, N. Itoh, V. E. Puchin, and E. N. Heifets, Phys. Rev. B **44**, 1499 (1991).
[11] V. E. Puchin, A. L. Shluger, K. Tanimura, and N. Itoh, Phys. Rev. B **47**, 6226 (1993).
[12] C.-R. Fu, L.-F. Chen, and K. S. Song, J. Phys.: Condens. Matter **11**, 5517 (1999).
[13] W. Moses, G. Bizarri, R. T. Williams, S. Payne, A. Vasil'ev, J. Singh, Q. Li, J. Grim, and W. Choong, IEEE Trans. Nucl. Sci. **59**, 2038 (2012).
[14] R. B. Murray and A. Meyer, Phys. Rev. **122**, 815 (1961).
[15] S. Payne, N. Cherepy, G. Hull, J. Valentine, W. Moses, and W.-S. Choong, IEEE Trans. Nucl. Sci. **56**, 2506 (2009).
[16] R. T. Williams and K. S. Song, J. Phys. Chem. Solids **51**, 679 (1990).
[17] A. M. Stoneham, J. Phys. C **7**, 2476 (1974).
[18] K. S. Song, A. M. Stoneham, and A. H. Harker, J. Phys. C **8**, 1125 (1975).
[19] N. Itoh and A. M. Stoneham, *Materials Modification by Electronic Excitation* (Cambridge University Press, Cambridge, UK, 2001).
[20] A. M. Stoneham, Modell. Simul. Mater. Sci. Eng. **17**, 084009 (2009).
[21] S. Kerisit, K. M. Rosso, B. D. Cannon, F. Gao, and Y. Xie, J. Appl. Phys. **105**, 114915 (2009).
[22] S. Nagata, K. Fujiwara, and H. Nishimura, J. Lumin. **47**, 147 (1990).
[23] H. Nishimura and S. Nagata, J. Lumin. **40-41**, 429 (1988).
[24] J. L. Gavartin, P. V. Sushko, and A. L. Shluger, Phys. Rev. B **67**, 035108 (2003).
[25] R. C. Baetzold and K. S. Song, J. Phys.: Condens. Matter **3**, 2499 (1991).
[26] S. E. Derenzo and M. J. Weber, Nucl. Instrum. Methods Phys. Res. A **422**, 111 (1999).
[27] J. F. Rivas-Silva, L. Rodríguez-Merino, M. Berrondo, and A. Flores-Riveros, Int. J. Quantum Chem. **77**, 785 (2000).
[28] P. V. Sushko, A. L. Shluger, and C. A. Catlow, Surf. Sci. **450**, 153 (2000).
[29] N. Govind, P. Sushko, W. Hess, M. Valiev, and K. Kowalski, Chem. Phys. Lett. **470**, 353 (2009).

[30]K. Momma and F. Izumi, J. Appl. Crystallogr. **44**, 1272 (2011).
[31]L. F. Pacios and P. A. Christiansen, J. Chem. Phys. **82**, 2664 (1985).
[32]F. Weigend and R. Ahlrichs, Phys. Chem. Chem. Phys. **7**, 3297 (2005).
[33]A. D. Becke, J. Chem. Phys. **98**, 1372 (1993).
[34]M. Valiev, E. Bylaska, N. Govind, K. Kowalski, T. Straatsma, H. V. Dam, D. Wang, J. Nieplocha, E. Apra, T. Windus *et al.*, Comput. Phys. Commun. **181**, 1477 (2010).
[35]E. C. M. Chen and W. E. Wentworth, J. Phys. Chem. **89**, 4099 (1985).
[36]A. Md Asaduzzaman and G. Schreckenbach, Theor. Chem. Acc. **122**, 119 (2009).
[37]P. E. Cade, A. M. Stoneham, and P. W. Tasker, Phys. Rev. B **30**, 4621 (1984).
[38]A. Song and R. T. Williams, *Self-Trapped Excitons*, Springer Series in Solid-State Sciences (Springer, New York, 1996).
[39]P. A. Rodnyi, *Physical Processes in Scintillators*, 1st ed. (CRC Press, Boca Raton, 1997).
[40]A. L. Shluger, L. N. Kantorovich, E. N. Heifets, E. K. Shidlovskaya, and R. W. Grimes, J. Phys.: Condens. Matter **4**, 7417 (1992).
[41]A. E. Mattsson, P. A. Schultz, M. P. Desjarlais, T. R. Mattsson, and K. Leung, Modell. Simul. Mater. Sci. Eng. **13**, R1 (2005).
[42]P. A. Schultz, SEQQUEST code, http:/dft.sandia.gov/Quest.
[43]J. P. Perdew and A. Zunger, Phys. Rev. B **23**, 5048 (1981).
[44]D. R. Hamann, Phys. Rev. B **40**, 2980 (1989).
[45]A. Fukuda, Phys. Rev. B **1**, 4161 (1970).
[46]L. S. Dang, Y. M. d'Aubigné, R. Romestain, and A. Fukuda, Solid State Commun. **26**, 413 (1978).
[47]A. D. Becke, J. Chem. Phys. **98**, 5648 (1993).